REVISTA Mundi
Engenharia, Tecnologia e Gestão
INSTITUTO FEDERAL Paraná

EFFECT OF WELDING POSITION ON THE MECHANICAL PERFORMANCE OF MANUAL METAL ARC WELDELD JOINTS VIA ANALYSIS OF VARIANCE

EFEITO DA POSIÇÃO DE SOLDAGEM NO COMPORTAMENTO MECÂNICO DE JUNTAS SOLDADAS MANUALMENTE A ARCO ELÉTRICO VIA ANÁLISE DE VARIÂNCIA

Rui Rosa de Morais Júnior[1]
Marcelo Xavier Guterres[2]
Alexandre Ferreira Galio[3]
Henara Lillian Costa[4]

Abstract: Positional welding is a common challenge in many manufacturing practices and the welding position can affect the mechanical properties of welded joints during manual metal arc welding. This work uses tensile tests to investigate the mechanical properties of welded joints, aiming to test the hypothesis of the influence of welding position on tensile strength, total displacement before rupture and plastic displacement before rupture. This hypothesis was tested for three different coated electrodes (AWS E6010, AWS E6013 and AWS E7018) and three welding positions (1G, 3G and 4G), accounting for nine types of specimens. For each type of specimen, ten repetitions were carried out. Analysis of Variance (ANOVA) was used to test the hypotheses. The welded joints using the welding position 1G presented higher rupture load and larger total displacement before rupture than the other positions.

Keywords: welding position. manual metal arc welding. tensile test. ANOVA.

Resumo: As posições de soldagem são um desafio comum em muitas práticas de fabricação e podem afetar as propriedades mecânicas das juntas soldadas durante a soldagem manual com arco metálico. Este trabalho utiliza testes de tração para investigar as propriedades mecânicas de juntas soldadas, visando testar a hipótese da influência da posição de soldagem na resistência à tração, deslocamento total antes da ruptura e deslocamento plástico antes da ruptura. Esta hipótese foi testada para três diferentes eletrodos revestidos (AWS E6010, AWS E6013 e AWS E7018) e três posições de soldagem (1G, 3G e 4G), representando nove tipos de amostras. Para cada tipo de amostra, dez repetições foram realizadas. A análise de variância (ANOVA) foi usada para testar as hipóteses. As juntas soldadas utilizando a posição de soldagem 1G apresentaram maior carga de ruptura e maior deslocamento total antes da ruptura do que as demais posições.

Palavras-chave: posição de soldagem. soldagem manual a arco elétrico. ensaio de tração. ANOVA.

[1] Mestre, Universidade Federal do Pampa, ruimoraisjr@gmail.com
[2] Doutor, Instituto Tecnológico da Aeronáutica, m.guterres@gmail.com
[3] Doutor, Universidade Federal do Pampa, galio.alexandre@gmail.com
[4] Doutora, Universidade Federal do Rio Grande, henaracosta@furg.br

1 INTRODUCTION

Welding is a key manufacturing process in applications such as joining, cutting and recovery of mechanical components. This broad range of applications implies that welding can be carried out under different environments, in elevated structures or even submerged in water (WAINER; BRANDI; MELLO, 2010). Under certain circumstances, the component cannot be removed for welding, so that the welder needs to adapt the welding practice to the convenient welding position.

Welding positions are classified as plane, horizontal, vertical and overhead. In manual metal arc welding (MMAW), welding position has a strong influence on the productivity and easiness of the welding operation (MASOUMI; SHAHRIARI, 2010). According to the American Society of Mechanical Engineers (ASME, 2010), the welding positions in butt welding are designated by one digit followed by one letter, so that the plane, horizontal, vertical and overhead positions are designated as 1G, 2G, 3G and 4G, respectively (Figure 1).

Figure 1. Welding positions for butt welding.

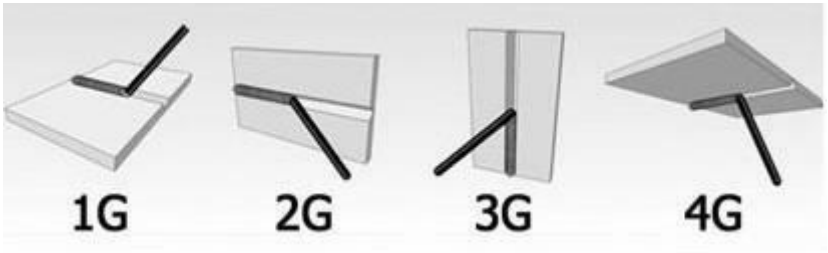

Font: Marques, Modenesi and Bracarense (2011).

Masoumi and Shahriari (2010) produced high strength steel welds using 1G and ascending 3G positions, evaluating their mechanical properties. They did not find statistically significant differences in the tensile properties depending on welding position. However, an adequate statistical model was not used to validate their findings. On the other hand, impact tests showed smaller impact energies for the ascending 3G position than for the 1G position.

The type of coating in the electrode can also affect the mechanical strength of a welded joint (CRESPO; FUENTES; SCOTTI, 2010). From an operational

point of view, rutile electrodes pose some advantages when compared with cellulosic and basic electrodes (FARIAS et al., 2004).

In view of the small amount of works in the literature using statistical analyses of the effects of welding position and coating type on the mechanical behaviour of welded joints, the present work aims to investigate the influence of the welding position (plane - 1G, vertical - 3G and overhead - 4G) on tensile strength and displacement before rupture when different coated electrodes (cellulosic - E6010, rutile - E6013, and basic - E7018) are used (ASME, 2010). Position 2G will not be tested because the difference in relation to position 3G was considered small and therefore not expected to change the mechanical properties significantly. Analysis of Variance (ANOVA) will be used to test the hypotheses.

2 MATERIALS AND METHODS

Different tests of hypothesis were carried out as indicated in Table 1, where H_0 is the null hypothesis, H_A is the alternative hypothesis and $\bar{y}_{i,j}$ is the average tensile strength obtained from the tensile tests in the welding position i (1G, 3G and 4G) with the electrode j (E6010, E6013, E7018). For the tests 1, 2 and 3, the j factor is fixed, whereas for the tests 4, 5 and 6, the i factor is fixed. The choice of the electrodes aimed at sampling the different types of coatings (rutile, cellulosic and basic) that are most widely used in industrial practice (ASME, 2010; SILVA; PEREIRA, 2010).

Table 1. Description of the tests of hypothesis.

Test 1	Test 2	Test 3
H_o: $\bar{y}_{1G,E1} = \bar{y}_{3G,E1} = \bar{y}_{4G,E1}$	H_o: $\bar{y}_{1G,E2} = \bar{y}_{3G,E2} = \bar{y}_{4G,E2}$	H_o: $\bar{y}_{1G,E3} = \bar{y}_{3G,E3} = \bar{y}_{4G,E3}$
H_A: $\bar{y}_{1G,E1} \neq \bar{y}_{3G,E1} \neq \bar{y}_{4G,E1}$	H_A: $\bar{y}_{1G,E2} \neq \bar{y}_{3G,E2} \neq \bar{y}_{4G,E2}$	H_A: $\bar{y}_{1G,E3} \neq \bar{y}_{3G,E3} \neq \bar{y}_{4G,E3}$
Test 4	Test 5	Test 6
H_o: $\bar{y}_{1G,E1} = \bar{y}_{1G,E2} = \bar{y}_{1G,E3}$	H_o: $\bar{y}_{3G,E1} = \bar{y}_{3G,E2} = \bar{y}_{3G,E3}$	H_o: $\bar{y}_{4G,E1} = \bar{y}_{4G,E2} = \bar{y}_{4G,E3}$
H_A: $\bar{y}_{1G,E1} \neq \bar{y}_{1G,E2} \neq \bar{y}_{1G,E3}$	H_A: $\bar{y}_{3G,E1} \neq \bar{y}_{3G,E2} \neq \bar{y}_{3G,E3}$	H_A: $\bar{y}_{4G,E1} \neq \bar{y}_{4G,E2} \neq \bar{y}_{4G,E3}$

Additional tests similar to those presented in Table 1 were carried out, where the values of $\bar{y}_{i,j}$ corresponded to the average total displacement before rupture and to the plastic displacement before rupture, respectively. Therefore, a total of 18 tests of hypothesis were carried out to answer the hypotheses investigated in the present work.

In order to carry out the test of hypothesis as described in Table 1, nine different welding operations were carried out (3 electrodes and 3 welding positions). Each welding condition was replicated 10 times, which was considered a reasonable number of repetitions within the time and material limitations. Other authors also consider 10 repetitions sufficient for comparison in welding processes using ANOVA (CORAINI; KOBAYASHI; GONÇALVES, 2011; TUSSET et al., 2008). For that, a special device was designed to obtain rectangular workpieces that were subsequently joined by welding (Figure 2). The device contains a workbench that ensures height regulation and 360º rotation, so that the workpieces could be joined by welding in the positions 1G (Figure 2a), 3G (Figure 2b) and 4G (Figure 2c).

Figure 2. Experimental device used in the welding operations: (a) 1G; (b) 3G; (c) 4G.

(a) (b) (c)

The welding joints were carried out for the union of two rectangular ASTM A36 steel workpieces with dimensions of 31.75mm x 50mm x 3.18mm. Butt welding without either grooving or gap between the plates was used to produce the unions. Manual Metal Arc Welding (MMAW) was carried out using a welding power supply model INVERT MXI-180ED. The technical specifications of the electrode brand (ESAB) were used, where 70A with reverse polarity (DC+) was

established for all the electrodes used. In addition, all electrodes were 2.5mm in diameter and were fixed at 45º in relation to the electrode holder. The welding process was performed by only one non-certified welder.

After welding, 90 specimens were produced for the tensile tests. In order to ensure that rupture would occur in the welded region, notches with depth of 4 mm were produced in the welds using a cutting disc (Figure 3a). In order to further increase the stress concentration at the bottom of the notches, sawing with a fine blade was used to produce a fine edge at the bottom region of the notches (Figure 3b).

Figure 3. Notching of the welded specimens: (a) initial notching with a cutting disc; (b) final sawing step at the bottom of the notch.

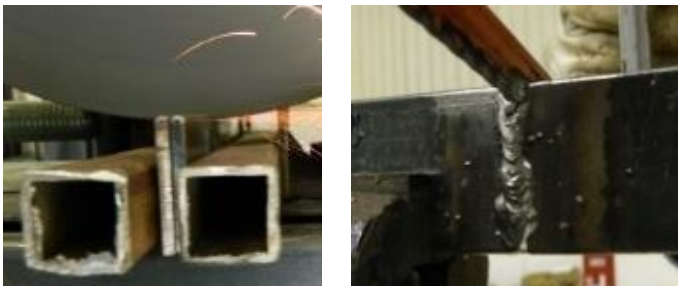

(a) (b)

A region with a width of 13 mm was marked around the welded region (Figure 4a) so that the specimens could be precisely positioned in the fixture device for the tensile tests (Figure 4b).

Figure 4. Positioning of the specimens for the tensile tests: (a) delimitation of the test area in the specimen; (b) specimen fixed in the tensile test grip.

(a) (b)

The tensile tests were carried out in an electromechanical machine model EMIC DL 10000. The load transducer has a maximum load capacity of 100 kN. The preload was 2 ± $2x10^{-2}$ kN and the pulling speed was 5 $mm.min^{-1}$.

A total of 90 specimens were tested (10 repetitions for 9 welding conditions) in order to perform all the tests of hypotheses listed in Table 1. The ANOVA technique was applied using a significance level of 5% (α = 0,05) with 21 degrees of freedom.

3 RESULTS AND DISCUSSION

Figure 5 shows the load versus displacement graphs obtained from the tensile tests. The nine welding conditions are the result of the following combinations: E6010 electrode / 1G position (Figure 5a), E6010 electrode / 3G position (Figure 5b), E6010 electrode / 4G position (Figure 5c), E6013 electrode / 1G position (Figure 5d), E6013 electrode / 3G position (Figure 5e), E6013 electrode / 4G position (Figure 5f), E7018 electrode / 1G position (Figure 5g), E7018 electrode / 3G position (Figure 5h), and E7018 electrode / 4G position (Figure 5i). All the repetitions are presented for each condition.

Average values and standard deviation values were calculated for all the variables $\bar{y}_{i,j}$ (rupture load, total displacement before rupture and plastic displacement before rupture), shown in Tables 2 to 4, respectively. During the averaging calculations, extreme values were excluded by removing the largest and the lowest values of the experimental observations in each set of results.

To obtain the rupture load, the standard collapse criterion was used, which corresponds to 20% of the maximum load. The total displacement before rupture was obtained directly from the x axis in the load versus displacement plot. The plastic displacement was calculated by plotting a line parallel to the elastic region and finding their intersection with the x axis.

Figure 5. Load versus displacement plots: (a) E6010/1G; (b) E6010/3G; (c) E6010/4G; (d) E6013/1G; (e) E6013/3G; (f) E6013/4G; (g) E7018/1G; (h) E7018/3G; (i) E7018/4G.

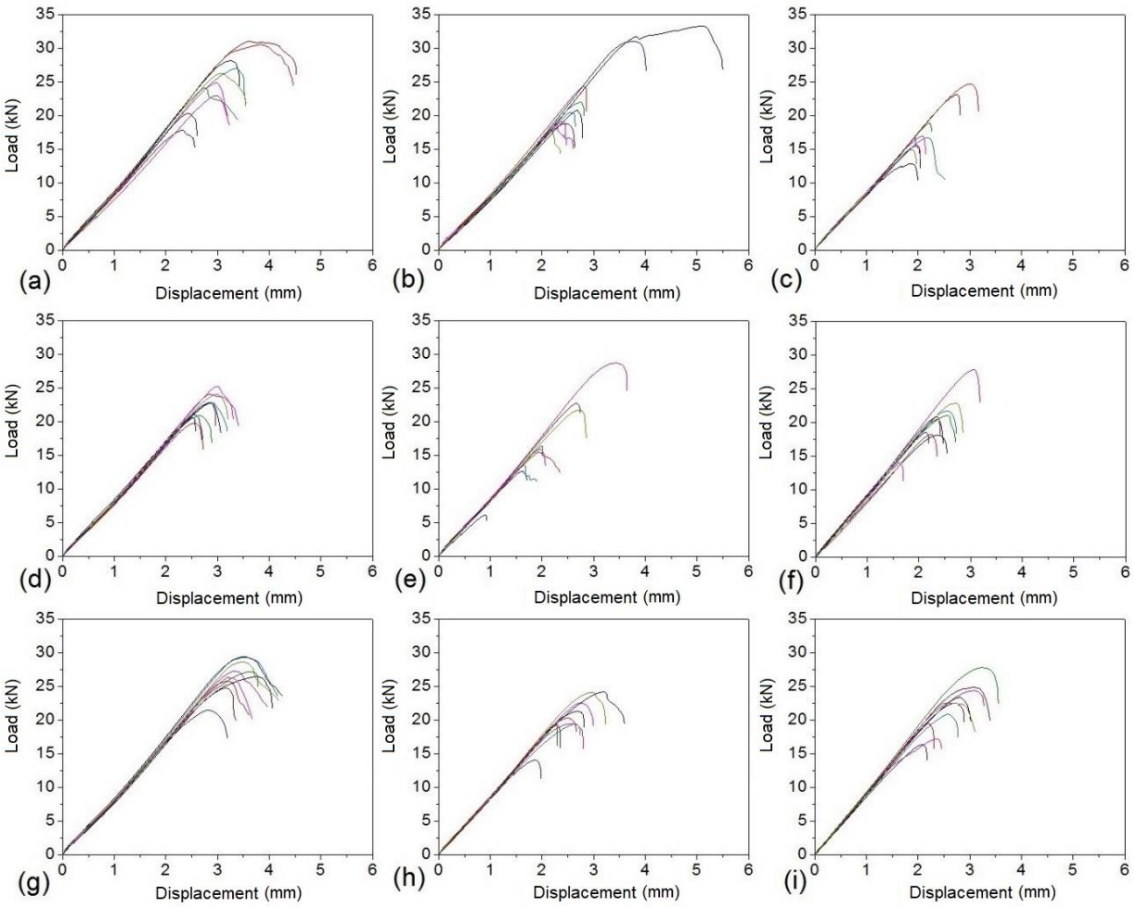

Table 2. Average ± standard deviations ($\bar{y}_{i,j} \pm S$) for the rupture load (kN).

	Welding position		
Electrode type	1G	3G	4G
AWS E6010 (cellulosic)	20.40 ± 2.55	17.51 ± 3.29	13.57 ± 2.4
AWS E6013 (rutile)	17.89 ± 1.11	13.75 ± 2.91	16.15 ± 1.39
AWS E7018 (basic)	21.57 ± 1.18	16.55 ± 1.45	17.51 ± 2.07

Table 3. Average ± standard deviations ($\bar{y}_{i,j} \pm S$) for the total displacement before rupture (mm).

	Welding position		
Electrode type	1G	3G	4G
AWS E6010 (cellulosic)	3.43 ± 0.52	2.85 ± 0.49	2.27 ± 0.28
AWS E6013 (rutile)	3.00 ± 0.22	2.27 ± 0.42	2.53 ± 0.22
AWS E7018 (basic)	3.85 ± 0.29	2.74 ± 0.31	2.90 ± 0.38

Table 4. Average ± standard deviations ($\bar{y}_{i,j} \pm S$) for the plastic displacement before rupture (mm).

	Welding position		
Electrode type	1G	3G	4G
AWS E6010 (cellulosic)	0.76 ± 0.34	0.57 ± 0.63	0.92 ± 0.86
AWS E6013 (rutile)	0.47 ± 0.09	0.96 ± 0.49	0.40 ± 0.14
AWS E7018 (basic)	1.02 ± 0.14	0.70 ± 0.32	0.85 ± 0.16

These values were used to test the hypotheses indicated in Table 1 using ANOVA. The results for the ANOVA tests are presented in Table 5.

Table 5. ANOVA results for the different welding conditions

Test	Description	Rupture Load		Total displacement		Plastic displacement		Critical F	α
		F	p	F	p	F	p		
1	E6010 - 1G,3G,4G	12.2	3.0E-04	13.7	1.6E-04	0.6	5.6E-01	3.5	5.0E-02
2	E6013 - 1G,3G,4G	8.9	1.6E-03	12.4	2.8E-04	8.3	2.2E-03		
3	E7018 - 1G,3G,4G	21.8	7.4E-06	26.9	1.6E-06	4.1	3.2E-02		
4	1G - E6010,E60	9.3	1.3E-03	10.7	6.2E-04	12.4	2.8E-04		
5	3G - E6010,E60	4.3	2.8E-02	4.5	2.3E-02	1.3	2.9E-01		
6	4G - E6010,E60	8.02	2.6E-03	8.89	1.6E-03	2.37	1.2E-01		

The analysis of Table 5 shows that for the level of significance α = 0.05 the null hypothesis must be rejected for all values of rupture load and total displacement because the calculated F are larger than the critical F= 3.5 obtained from Fisher-Snedecor's distribution, having 2 degrees of freedom in the numerator and 21 degrees of freedom in the denominator. Therefore, the null hypothesis must be rejected for these variables, i.e., the tested average values for rupture load and total displacement are significantly different. These results are confirmed by p-values below α, which is the largest value for which the null hypothesis is rejected.

A linear regression was calculated using the average values for total displacement in x and the average values for the rupture load in y. This gave a Pearson correlation coefficient r = 0.9853, showing a very strong correlation between the two variables. This probably occurs because the plots showed a very large linear region following Hooke´s law. The fact that both the rupture load and the total displacement showed similar statistical tendencies mirrors this strong correlation.

On the other hand, for the plastic displacement, the values of F and p for the tests 1, 5 and 6, whereas the null hypothesis is rejected for the tests 2, 3 and 4. However, it must be pointed out that the method used to calculate the plastic displacement was not very precise because it measured the displacement of the test claws and not real elongation of the welded region. The use of extensometers to measure the displacements directly from the specimens should improve the precision of the results obtained and this is a topic of future investigation.

The main goal of the present study was to present a statistically robust methodology to investigate the mechanical behavior of welded joints. The device designed for the welding operations was successful to control precisely the welding position. The tests were able to show with statistical confidence that the 1G position resulted in the highest values of rupture load and total displacement for all the electrode types. Comparing the positions 3G and 4G, the overhead position resulted in lower rupture loads and lower total displacements only for the cellulosic electrode.

As the welding position moves from flat to vertical and then to overhead the heat input lowers (MASOUMI; SHAHRIARI, 2010). It has been proposed by Sarafan et al. (2012) that lower heat inputs lead to higher cooling rates, affecting the microstructure. Cellulosic electrodes contain a large moisture content, typically 4 to 5%. Burning of the cellulose in conjunction with the moisture produces a large amount of hydrogen. The combination of overhead position (highest cooling rate) with a cellulosic electrode may increase the susceptibility to cold cracking due to higher levels of diffusible hydrogen remaining in the weld metal after welding. Sarafan et al. (2012) also suggest that welding position can

affect residual stresses induced by welding, but highlight that this point needs further investigation.

For this reason, in the 4G position, the use of a basic electrode resulted in the highest rupture load and total displacement. The electrode coating is of fundamental importance to define the mechanical properties of a welded joint (ADEYEYE; OYAWALE, 2009). Basic electrodes contains no cellulose and, if correctly handled before welding, negligible moisture should be present, which results in superior microstructure and higher mechanical properties in the welded region (LIU; OLSON, 2003).

Therefore, the combined use of a basic electrode (E7018) in the plane position (1G) resulted in the highest values of rupture load and total displacement for all the conditions tested. The lower levels of hydrogen in the welded material provided by the basic electrode combined with the lower cooling rates obtained in the 1G position should indeed result in superior mechanical properties.

In the 3G position, the cellulosic electrode presented higher rupture load and total displacement. This is probably due to the fact that the decomposition of the cellulosic coating results in large penetration and good control of the weld pool (reduced tendency to pool collapse). For this reason cellulosic electrodes are indicated for root welding operations (GHOMASHCHI; COSTIN; KURJI, 2015).

Regarding the rutile electrodes despite being known to have excellent operability, this did not translate into better resistance results. This may be related to the fact that the specifications of the 6013 and 6010 electrodes indicate a lower tensile strength than the 7018 electrode. As the 6010 cellulosic electrode has a higher penetration than the 6013 rutile electrode, the 6013 had the worst results at positions 1G and 3G. In the 4G position, the 6010 electrode presented the worst result, probably due to the gravity force that decreases the penetration of the weld, which suggests to be a more suitable electrode for welding in the 1G position.

4 CONCLUSIONS

This work used a statistically robust methodology to investigate how the welding position and the type of electrode coating influence mechanical properties of plain carbon steel joints produced by manual metal arc welding. ANOVA tests showed that the average values for rupture load and total displacement were significantly different. The same was not true for the plastic displacement, which probably requires the use of more precise methods to measure displacement. The results allowed to conclude that:

- The use of a basic electrode E7018 combined with 1G position results in the highest values of rupture load and total displacement;
- In the 3G position, the cellulosic electrode E6010 resulted in the best mechanical properties;
- In the 4G position, the highest values of rupture load and total displacement were obtained by the basic electrode E7018;
- The rutile electrode E6013 showed the worst results of rupture load for positions 1G and 3G;
- The cellulosic electrode E6010 showed the worst results of rupture load for position 4G.

REFERENCES

ADEYEYE, A. D.; OYAWALE, F. A. Weld-metal property optimization from flux ingredients through mixture experiments and mathematical programming approach. Materials Research, v. 12, n. 3, p. 339-343, 2009.

ASME – SFA-5.1/SFA-5.1M. Specification for carbon steel electrodes for shielded metal arc welding, 2010.

CORAINI, R.; KOBAYASHI, Y.; GONÇALVES, G. M. B. Influência do tipo de chanfro, tecimento, e sentido de laminação na distorção angular em soldagem gmawp robotizada de alumínio. Soldagem e Inspeção, v. 16, n. 2, p. 123-136, 2011.

CRESPO; A. C.; FUENTES, R. F.; SCOTTI, A. The Influence of Calcite, Fluorite, and Rutile on the Fusion-Related Behavior of Metal Cored Coated Electrodes for

Hardfacing. Journal of Materials Engineering and Performance, v. 19, n. 5, p. 685 - 692, 2010.

FARIAS, J. P.; SCOTTI, A.; BÁLSAMO, P. S. de S.; SURIAN, E. The Effect of Wollastonite on Operational Characteristics of AWS E6013 Electrodes. J. of the Braz. Soc. of Mech. Sci. & Eng, v. 26, n. 3, p. 317-322, 2004.

GHOMASHCHI, R.; COSTIN, W.; KURJI, R. Evolution of weld metal microstructure in shielded metal arc welding of X70 HSLA steel with cellulosic electrodes: A case study. Materials Characterization, v. 107, p. 317-326, 2015.

LIU, S.; OLSON, D. L. Weld metal design: From flux coating to microstructure. ASM International, Materials Park, 2003.

MARQUES, P. V., MODENESI, P. J., BRACARENSE, A. Q. Soldagem: fundamentos e tecnologia. Belo Horizonte - Brasil: Editora UFMG, 2011.

MASOUMI, F.; SHAHRIARI, D. Effects of Welding Positions on Mechanical Properties and Microstructure in Weld Metal of High Strength Steel. Advanced Materials Research, v. 83-86, p 1121-1127, 2010.

SARAFAN, S.; GHAINI, F. MALEK; RAHIMI, E. Effects of Welding Direction and Position on Susceptibility to Weld Metal Transverse Cracking in Welding High-Strength Pipeline Steel with Cellulosic Electrodes. Welding Journal, 2012.

SILVA, B. E. S.; PEREIRA, W. X. Estudo da influência de eletrodos revestidos nas características geométricas e metalúrgicas das juntas soldadas pelo processo SMAW. VI Congresso Nacional de Engenharia Mecânica, Campina Grande, Brasil, 2010.

TUSSET, A. M.; CASTRO, E. C.; PAULA FILHO. P. L.; TESSARO, A. P. Análise Comparativa entre a Solda MIG Robotizada e a Solda MIG Manual Através da Análise de Variância. In: 7º Congresso Temático de Dinâmica, Controle e Aplicações-UNESP, Área. 2008. p. 01-07.

WAINER, E., BRANDI, S. D., MELLO, F. D. H. Soldagem: Processo e Metalurgia. São Paulo - Brasil: Editora Blucher, 2010.

Enviado em: 30 nov. 2018
Aceito em: 15 dez. 2019
Editor responsável: Mateus das Neves Gomes